

# Organotetrel Chalcogenide Clusters: Between Strong Second-Harmonic and White-Light Continuum Generation

Nils W. Rosemann,<sup>‡,§,||</sup> Jens P. Eußner,<sup>†,||</sup> Eike Dornsiepen,<sup>†,||</sup> Sangam Chatterjee,<sup>‡,§</sup> and Stefanie Dehnen<sup>\*,†,||</sup>

<sup>†</sup>Fachbereich Chemie und Wissenschaftliches Zentrum für Materialwissenschaften (WZMW), Philipps-Universität Marburg, Hans-Meerwein-Straße 4, DE-35043 Marburg, Germany

<sup>‡</sup>Fachbereich Physik und Wissenschaftliches Zentrum für Materialwissenschaften (WZMW), Philipps-Universität Marburg, Renthof 5, DE-35032 Marburg, Germany

<sup>§</sup>Institute of Experimental Physics I, Justus-Liebig-University Giessen, DE-35392 Giessen, Germany

## S Supporting Information

**ABSTRACT:** Highly directional white-light generation was recently reported for the organotin sulfide cluster  $[(\text{StySn})_4\text{S}_6]$  (Sty = *p*-styryl). This effect was tentatively attributed to the amorphous nature of the material in combination with the specific combination of an inversion-symmetry-free T/E cluster core (T = tetrel, E = chalcogen) with the attachment of ligands that allow  $\pi$  delocalization of the electron density. Systematic variation of T and the organic ligand (R) that runs from T = Si through Ge to Sn and from R = methyl through phenyl and *p*-styryl to 1-naphthyl provides a more comprehensive view. According to powder X-ray data, only  $[(\text{PhSi})_4\text{S}_6]$  is single-crystalline among the named combinations. Here we demonstrate the fine-tuneability of the nonlinear response, i.e., changing from white-light generation to second-harmonic generation as well as controlling the white-light properties. These are investigated as a function of T,  $\pi$  delocalization of the electron density within R, and the order within the molecular solids.

Light-converting materials are continuously being developed for a multitude of applications, including advanced phosphors for bright white-light emission in light-emitting diodes.<sup>1</sup> These are nowadays omnipresent in diffuse illumination and display applications. Other light-converting materials target nonlinear optical processes such as second-harmonic generation (SHG).<sup>2</sup> Here, typically coherent laser radiation is upconverted into light of half the wavelength of the incident radiation. This is commonly achieved in crystalline materials lacking inversion symmetry.<sup>3a</sup> Microscopically, this enables the fundamental incident light to introduce a nonlinear polarization in the crystal. For phase-matching conditions, i.e., when the refractive index of fundamental and second-harmonic light are identical, both can exit the nonlinear medium and may later be separated.<sup>3b</sup> Currently, the search for advanced light conversion media is aiming at increased conversion efficiencies and extended accessible frequency regimes.<sup>4</sup>

Another class of highly nonlinear light-converting materials enhance effects such as self-phase modulation. These are used in extreme nonlinear processes such as the generation of highly

brilliant (i.e., directional) broadband supercontinua. However, this process commonly requires intense, short-pulsed laser sources, confining their use to mostly scientific applications.<sup>5</sup>

In the course of our current research on tetrel chalcogenide hybrid compounds, clusters, and functional networks,<sup>6</sup> we recently showed that the organotin sulfide cluster compound  $[(\text{StySn})_4\text{S}_6]$  (Sty = *p*-styryl,  $4\text{-H}_2\text{C}=\text{CH}-\text{C}_6\text{H}_4$ ) produces spectrally broadband and highly brilliant white light. The observed vast optical nonlinearity even allows this process for low-fluence steady-state illumination generated from cost-effective near-infrared continuous-wave laser diodes. Tentatively, the white-light generation was identified as emission from coherently accelerated electrons in the delocalized  $\pi$ -electron system of the organic ligands combined with a strong transition dipole that is provided by the tetrel chalcogenide cluster core and a lack of phase matching.<sup>7</sup>

For a more comprehensive view of the nonlinear optical response, we studied the effect of slight variations of the system. For this, we prepared two series of compounds of the general formula  $[(\text{RT})_4\text{S}_6]$  (R = organic ligand; T = Si, Ge, Sn). All of these compounds were expected to exhibit (very) strong nonlinear optical properties, as they have similar compositions and structures as the proof-of-principle compound, included in this study as compound 3 for comparison.

One series addressed the effect of the ligands on the  $[(\text{RSn})_4\text{S}_6]$  scaffold. The ligands were varied from R = Me (1)<sup>8a</sup> through R = 1-naphthyl (Np) (2) and Sty (3)<sup>7</sup> to R = Ph (4)<sup>8b</sup> for exploration of the impact of the presence and the nature of the  $\pi$ -electron system. For this, it was either completely absent (Me) or decreased in size (Np → Sty → Ph). Changing the ligand particularly changes the intermolecular interactions, including the tendency of the solid material to exhibit no, short-range, or long-range order, which determines its amorphousness versus crystallinity. The second series addressed the composition of the inorganic cluster core. This affects the optical gap of the clusters, starting out from the Sn/S combination in 4 through Ge/S (5) to Si/S (6).<sup>9</sup> Overall, the two sample series reveal (i) whether and how the T/E/R

Received: October 19, 2016

Published: November 29, 2016

combination affects the orderliness or potential crystallization and (ii) how this affects the nonlinear optical properties.

All of the compounds were obtained upon reaction of the respective organotetrel halides  $RTCl_3$  with sodium sulfide in an acetone/water solvent mixture or tetrahydrofuran at room temperature, with the formation of NaCl being the driving force for the cluster formation. Except for compound **6**, the compounds were obtained as amorphous powders under a large variety of reaction and crystallization conditions tested to date.<sup>2</sup> Hence, the molecular structures of the latter were elucidated via density functional theory (DFT) calculations (see the Supporting Information). According to these, all of the compounds are based on a heteroadamantane-type  $[T_4S_6]$  scaffold, which is energetically favored over the “double-decker”-type isomer by 19.2–36.4 kJ/mol (see Table S1 and the Supporting Information). The organic substituents point away from the center of the inorganic cluster core in pseudotetrahedral fashion. As an exception, compound **6** could be obtained as single crystals. Thus, the structure of this compound was determined by single-crystal X-ray diffraction, thereby confirming the previous prediction for it.<sup>8c</sup> The structure was solved and refined in the monoclinic space group  $P2_1/c$  with  $Z = 4$  (see Figure 1 and the Supporting

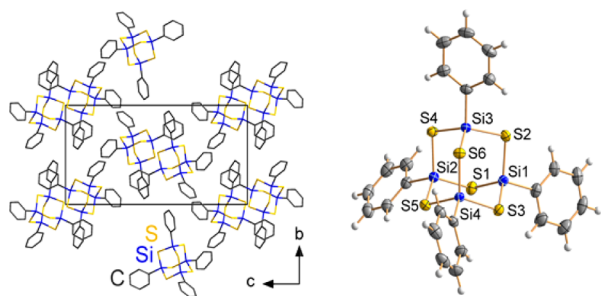


**Figure 1.** Fragment of (left) the crystal structure (wire representation, shown without H atoms) and (right) the molecular structure (ellipsoids drawn at the 70% probability level) of  $[(PhSi)_4S_6]$  (**6**) according to X-ray diffraction studies. Selected structural parameters [Å, deg]: Si–S, 2.1184(5)–2.1476(5); C–Si, 1.854(1)–1.855(1); Si–S–Si, 102.86(2)–104.25(2); S–Si–S, 111.29(2)–113.27(2); C–Si–S, 103.85(5)–108.50(5).

Information). In agreement with DFT calculations, the molecular structure of **6** is based on an inversion-free heteroadamantane-type inorganic scaffold with (idealized)  $T_d$  symmetry. The actual crystallographic symmetry is reduced by different orientations of the organic groups and by slight deformations of the inorganic core.

Next, we investigated the nonlinear optical properties of the compounds. The samples were kept under high-vacuum conditions during laser irradiation. For excitation, a continuous-wave diode laser operating at a central wavelength of 980 nm was used. The optical power of 200 mW was focused on the sample in a confocal setup featuring a reflective microscope objective to avoid any chromatic aberrations (see the Supporting Information). This setup yielded a spot diameter of less than 10  $\mu\text{m}$  on the sample. For detection, a Czerny–Turner-type spectrometer equipped with a thermoelectrically cooled back-illuminated deep-depletion Si-charge-coupled device camera was used. Residual scattered pump laser was attenuated using a heat-absorbing glass filter (Schott KG3).

Characteristic spectra of the first sample series (compounds 1–4) are given in Figure 2. Clearly, the nature and extent of the

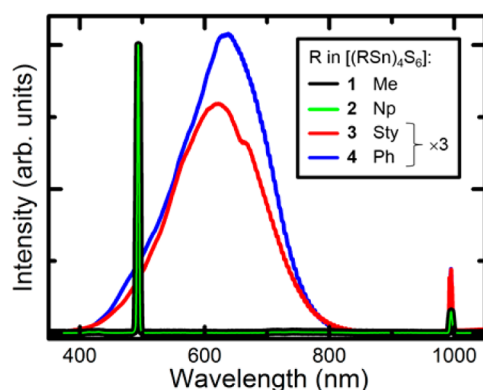


**Figure 2.** Emission spectra measured for an excitation wavelength of 980 nm. Compounds **1** (black) and **2** (green) exhibit intense SHG. Compounds **3** (red) and **4** (blue) exhibit strong white-light emission (scaled by a factor of 3).

$\pi$ -electron system crucially influence the optical nonlinearity. Compounds **3** and **4** show pronounced white-light emission, while compounds **1** and **2** show intense SHG. The latter requires phase matching (which is not a precondition for white-light emission). Hence, the optical experiments infer a certain degree of order in the powders obtained for **1** and **2**. In **1**, both the low steric demand and the low flexibility of the ligand seem to allow for order—which can even lead to the formation of single crystals<sup>8a</sup>—although it is not visible in the X-ray diffraction diagrams of the powder studied herein (Figure S3). In the case of **2**, the pronounced  $\pi$ – $\pi$ -stacking capability of the Np ligands apparently causes a relatively high degree of order in the amorphous powder. Hence, the two ligands, although significantly different in size and electronic nature, provoke similar nonlinear responses.

The situation changes upon attachment of ligands with a medium-sized extension of the  $\pi$ -electron system. Obviously, an effective intermolecular interaction does not take place between the cluster molecules in **3** ( $R = \text{Sty}$ ), which we attribute to both the reduced  $\pi$ -stacking capability compared with Np ligands and the higher conformational flexibility of the Sty ligands compared with all of the other ligands involved herein. The smallest  $\pi$ -electron system in this series is present in the Ph groups in compound **4**. Like the Sty ligands in **3**, they hamper any intermolecular order when attached to the  $[Sn_4S_6]$  core. Hence, phase matching is ruled out, and the nonlinear optical response changes from SHG to white-light generation.

The subtle yet crucial role of microscopic molecular order is further underlined by the slightly reduced white-light generation in **3** compared with **4**. In these compounds, the delocalization of the  $\pi$ -electron system is virtually identical. Nevertheless, the Sty ligands in **3** provide an increased potential for dispersive interactions between neighboring molecules and thus a potentially higher degree of order in the material, without reaching long-range order or crystallinity. Thus, the strength of the nonlinear optical response might in turn be used as a measure of the degree of intermolecular order in a macroscopically amorphous compound.

The strong nonlinear response found for all four compounds underlines the efficient enhancement of the nonlinearity by the transition dipole moment of the cluster core. Hence, even compound **1**, with its comparatively small electronic system, exhibits SHG, as the Me groups are in close proximity to the inorganic core.

The second group of samples comprises compounds **4**, **5**, and **6**. Here the inorganic cluster core is varied while the Ph ligands, which proved as most suitable for white-light generation in the first series, remain unchanged. In striking difference to the other two Ph-decorated compounds, **6** was obtained as clear and sizable single crystals (Figure S5). This difference in appearance is directly reflected in the measured spectra shown in Figure 3. SHG is exclusively observed for the crystalline compound whereas the other two exhibit broadband white-light emission, in perfect agreement with the assumption given above.

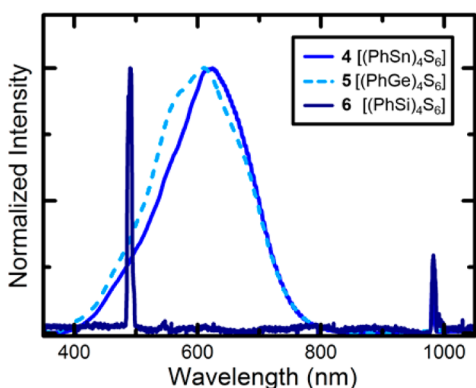


**Figure 3.** Spectra measured for an excitation wavelength of 980 nm. The amorphous compounds **4** (blue) and **5** (light blue, dashed) exhibit strong white-light emission. The crystalline compound **6** (dark blue) exhibits strong SHG.

The fact that Ph ligands, which perfectly exclude crystallization in the case of compounds **4** and **5**, do allow for the longer-range order in a crystal lattice in **6**, can be attributed to the different relative sizes of the three components T, E, and R. Obviously, four Ph ligands match well the steric demands of the  $[\text{Si}_4\text{S}_6]$  scaffold to form a stable crystal structure with interdigitating Ph groups that, however, do not feature any typical  $\pi$ -stacking orientations with respect to each other. In contrast, a suitable crystal lattice seems to be lacking in the T/E/R = Sn/S/Ph and Ge/S/Ph combinations in **4** and **5**, respectively.

Comparison of the spectra of **4** and **5** reveals a blue shift of the maximum and of the high-energy flank when Sn is replaced with Ge. The white-light spectrum in both compounds is limited by reabsorption from the fundamental electronic transition of the cluster core. In accordance with the band gaps of  $\text{SnS}_2$  and  $\text{GeS}_2$  (2.18–2.44 eV<sup>9</sup> and 3.2 eV,<sup>10</sup> respectively), the reabsorption limit in compound **5** is blue-shifted relative to that in **4**. This is confirmed by UV/vis absorption spectroscopy (Figure S2). The white-light spectrum in both compounds is limited by reabsorption from the fundamental electronic transition of the cluster core.<sup>1</sup>

In conclusion, we have investigated the nonlinear optical response of two series of organotetrel chalcogenide cluster compounds of the general formula  $[(\text{RT})_4\text{S}_6]$  (R = Me, Np, Sty, Ph; T = Si, Ge, Sn) and identified prerequisites for either SHG or white-light generation. Variation of the ligand R showed that for a given size of the inorganic  $[\text{T}_4\text{S}_6]$  cluster core, white-light generation is observed when R efficiently prevents any ordering of the solid compound. Opening a capability of ordering via intermolecular interactions reduces the efficiency of the white-light generation. Allowing for more order—in the

case of T = Sn realized by small Me ligands or enhanced  $\pi$ -stacking capability—changes the nonlinear response from white-light generation to SHG. This was ultimately proven by SHG observed for a long-range-ordered system of a single crystal. The conditions for long-range order to occur are suitable relative sizes of the T, E, and R components and/or pronounced  $\pi$ -stacking capability.

For comparable systems that show the same type of nonlinear response, it was shown that changing T from Sn to Ge results in a blue shift of the absorption edge and thus in a blue shift of the white-light emission. Both findings underline the white-light generation mechanism proposed in previous studies.

## ■ ASSOCIATED CONTENT

### Supporting Information

The Supporting Information is available free of charge on the ACS Publications website at DOI: 10.1021/jacs.6b10738.

Further information on synthesis and characterization (NMR, TGA/DSC,  $\mu$ RFA, PXRD, UV/vis, IR) (PDF) Crystallographic data for **6** (CIF)

## ■ AUTHOR INFORMATION

### Corresponding Author

\*dehnen@chemie.uni-marburg.de

### ORCID

Nils W. Rosemann: 0000-0002-7663-0397

Stefanie Dehnen: 0000-0002-1325-9228

### Author Contributions

<sup>||</sup>N.W.R., J.P.E., and E.D. contributed equally.

### Notes

The authors declare no competing financial interest.

## ■ ACKNOWLEDGMENTS

This work was supported by the Deutsche Forschungsgemeinschaft within the framework of Grant GRK1782. We thank Jan Christman for his help with the synthesis and Vanessa Dahmen for her help with the spectroscopic experiments.

## ■ REFERENCES

- (1) (a) Mueller-Mach, R.; Mueller, G.; Krames, M. R.; Höpfe, H. A.; Stadler, F.; Schnick, W.; Juestel, T.; Schmidt, P. *Phys. Status Solidi A* **2005**, *202*, 1727–1732. (b) Nakamura, S. *Proc. SPIE* **1997**, *3002*, 26–35. (c) Kimme, F.; Brick, P.; Chatterjee, S.; Khanh, T. *Appl. Opt.* **2013**, *52*, 8779–8788.
- (2) (a) Franken, P.; Hill, A.; Peters, C.; Weinreich, G. *Phys. Rev. Lett.* **1961**, *7*, 118–119. (b) Petrov, V.; Ghotbi, M.; Kokabee, O.; Esteban-Martin, A.; Noack, F.; Gaydardzhiev, A.; Nikolov, L.; Tzankov, P.; Buchvarov, I.; Miyata, K.; Majchrowski, A.; Kityk, I. V.; Rotermund, F.; Michalski, E.; Ebrahim-Zadeh, M. *Laser Photonics Rev.* **2010**, *4*, 53–98.
- (3) (a) Nikogosyan, D. N. *Nonlinear Optical Crystals: A Complete Survey*; Springer: Berlin, 2005. (b) Boyd, R. W. *Nonlinear Optics*, 3rd ed.; Elsevier Science: New York, 2008.
- (4) (a) Green, M. L. H.; Marder, S. R.; Thompson, M. E.; Bandy, J. A.; Bloor, D.; Kolinsky, P. V.; Jones, R. J. *Nature* **1987**, *330*, 360–362. (b) Alford, W. J.; Smith, A. V. *J. Opt. Soc. Am. B* **2001**, *18*, 524. (c) Muhammad, S.; Al-Sehemi, A. G.; Irfan, A.; Chaudhry, A. R. *J. Mol. Graphics Modell.* **2016**, *68*, 95–105. (d) Kanseri, B.; Bouillard, M.; Tualle-Brouri, R. *Opt. Commun.* **2016**, *380*, 148–153. (e) Canagasabay, A.; Corbari, C.; Gladyshev, A. V.; Liegeois, F.; Guillemet, S.; Hernandez, Y.; Yashkov, M. V.; Kosolapov, A.; Dianov, E. M.; Ibsen, M.; Kazansky, P. G. *Opt. Lett.* **2009**, *34*, 2483–2485.

(5) (a) Alfano, R. R. *The Supercontinuum Laser Source*; Springer: New York, 2016. (b) Birks, T. A.; Wadsworth, W. J.; Russell, P. S. J. *Opt. Lett.* **2000**, *25*, 1415–1417. (c) Husakou, A. V.; Herrmann, J. *Phys. Rev. Lett.* **2001**, *87*, 203901.

(6) (a) Santner, S.; Heine, J.; Dehnen, S. *Angew. Chem., Int. Ed.* **2016**, *55*, 876–893. (b) Thiele, G.; Franzke, Y.; Weigend, F.; Dehnen, S. *Angew. Chem., Int. Ed.* **2015**, *54*, 11283–11288. (c) Eußner, J. P.; Dehnen, S. *Chem. Commun.* **2014**, *50*, 11385–11388. (d) Bron, P.; Johansson, S.; Zick, K.; Schmedt auf der Günne, J.; Dehnen, S.; Røling, B. *J. Am. Chem. Soc.* **2013**, *135*, 15694–15697. (e) Lin, Y.; Massa, W.; Dehnen, S. *J. Am. Chem. Soc.* **2012**, *134*, 4497–4500. (f) Fard, Z. H.; Halvagar, M. R.; Dehnen, S. *J. Am. Chem. Soc.* **2010**, *132*, 2848–2849.

(7) Rosemann, N. W.; Eußner, J. P.; Beyer, A.; Koch, S. W.; Volz, K.; Dehnen, S.; Chatterjee, S. *Science* **2016**, *352*, 1301.

(8) (a) Crystal structure of **1**: Kobelt, D.; Paulus, E. F.; Scherer, H. *Acta Crystallogr., Sect. B: Struct. Crystallogr. Cryst. Chem.* **1972**, *28*, 2323. (b) Synthesis of **4**: Berwe, H.; Haas, A. *Chem. Ber.* **1987**, *120*, 1175–1182. (c) Synthesis of **6**: Fehér, F.; Lüpshen, R. *Z. Naturforsch., B: J. Chem. Sci.* **1971**, *26b*, 1191–1192.

(9) (a) Hu, S.; Song, G.; Li, W.; Peng, Y.; Jiang, L.; Xue, Y.; Liu, Q.; Chen, Z.; Hu, J. *Mater. Res. Bull.* **2013**, *48*, 2325. (b) Panda, S.; Antonakos, A.; Liarokapis, E.; Bhattacharya, S.; Chaudhuri, S. *Mater. Res. Bull.* **2007**, *42*, 576. (c) Deshpande, N.; Sagade, A.; Gudage, Y.; Lokhande, C.; Sharma, R. *J. Alloys Compd.* **2007**, *436*, 421.

(10) Nikolic, P. M.; Popovic, Z. V. *J. Phys. C: Solid State Phys.* **1979**, *12*, 1151.